Light trapping by hydrothermally deposited zinc oxide nanostructures with high haze ratio

Shahbaz Khan [a], Shahzada Qamar Hussain [a], Doyeon Hwang [b], S. Velumani [c], Hyoyoung Lee [a,b,*]

[a] Department of Energy Science, Sungkyunkwan University, Suwon 440-746, Korea
[b] National Creative Research Initiative, Center for Smart Molecular Memory, Department of Chemistry, Sungkyunkwan University, 2066 Seoburo, Jangan-Gu, Suwon, Gyeonggi-Do 440-746, Korea
[c] Department of Electrical Engineering (SEES), CINVESTAV-IPN, Avenida IPN 2508, San Pedro Zacatenco, Mexico D.F., Mexico

ARTICLE INFO

ABSTRACT

Surface morphology of the front transparent conductive oxide film is critical to achieve high short circuit current density in amorphous silicon (a-Si) thin film solar cells due to its high electrical conductivity and transparency accompanying excellent light scattering. Here, we present a low cost hydrothermal route to deposit zinc oxide nanoflowers and nanoflakes exhibiting low sheet resistance and high haze ratio for a-Si thin film solar cells. Zinc oxide nanoflowers and nanoflakes with various aspect ratios were grown on standard fluorine doped tin oxide glass by modulating growth time and hydrogen doping. Zinc oxide nanoflowers and nanoflakes exhibited superior light scattering compared to conventional zinc oxide nanostructures due to a higher surface area and displayed a higher haze ratio compared to the commercially available fluorine doped tin oxide films. Moreover, electrical conductivity and crystallinity of zinc oxide nanoflowers and nano-flakes could be enhanced by annealing in hydrogen atmosphere at 350 °C. We also observed that zinc oxide nanoflowers with high aspect ratio showed high transmittance spectra for a wider wavelength range. Therefore, we propose a low cost scale up synthesis of high haze ratio zinc oxide nanoflowers and nanoflakes for the enhanced performance of thin film solar cells.

1. Introduction

Over the past decade, amorphous silicon (a-Si) based thin film solar cells (TFSCs) have attracted considerable attention for the future high efficiency large-area and low cost photovoltaic devices [1]. The front transparent conductive oxide films (TCOs) play a vital role to improve the performance of a-Si TFSCs due to their high transmittance, low resistivity and excellent scattering properties [1–3]. Various TCO films, such as fluorine doped tin oxide (FTO) [4], aluminum doped zinc oxide (ZnO:Al) [5], boron doped zinc oxide (ZnO:B) [6] and gallium doped zinc oxide (ZnO:Ga) [7], have been used for the fabrication of a-Si TFSCs. The above mentioned TCOs are mostly fabricated by magnetron sputtering [8] or metal organic-chemical vapor deposition [9], which are expensive processes. Moreover, the front TCO films are separately textured by wet chemical and dry etching process for light trapping. Recently, alternative TCO films with better light scattering are being investigated. Chemically deposited ZnO nanostructures like nanorod, nanoflowers (NF$_S$) and nano-flakes (NF$_K$) arrays with superior chemical, electronic and

---

* Corresponding author at: Department of Energy Science, Sungkyunkwan University, Suwon, 440-746, Korea.
E-mail address: hyoyoung@skku.edu (H. Lee).

optical properties have been extensively studied for the chemical sensors [10], piezoelectric devices [11], field-emitting devices [12], and solar cells [6] applications. Low cost ZnO based nanorods, NF$_S$ and NF$_K$ [13] are proposed for light scattering in a-Si thin solar cells [14] and dye sensitized [15] solar cells.

ZnO based nanostructures can be deposited by various methods including pulsed laser deposition [16], chemical vapor deposition [17], electro-chemical deposition [18] and hydrothermal chemical [19] processes. The hydrothermal chemical process is preferred due to its simplicity, large area applications and low cost deposition. Kilic et al. reported the fabrication of 3-D ZnONF$_S$ structures for high quantum and photocurrent efficiency in dye sensitized solar cells [20]. Umar et al. reported hydrothermally grown ZnONF$_S$ for the environmental remediation and clean energy applications [19]. Nowak et al. recently proposed ZnO nanorod arrays as light trapping structures in a-Si thin-film solar cells [14]. Electrical conductivity of metal oxides can be improved by the hydrogenation or annealing in hydrogen environment [21]. Chris et al. reported that hydrogen (H) ion acts as a source for enhancing conductivity in ZnO. Since H-ion is stable and the lowest-energy state for all Fermi-level positions and can be incorporated in high concentrations as a shallow donor in ZnO [22,23]. This behavior is very different from hydrogen used in other semiconductors, in which it only acts as a compensating center and always reduces the conductivity. This prediction was experimentally confirmed by Yang et al. [24]. Although, various reports related to hydrothermally deposited ZnONF$_S$ and ZnONF$_K$ for dye-sensitized solar cells are available [15], a very few reports for the use of ZnONF$_S$ and ZnONF$_K$ with high haze ratio for the a-Si based thin film solar cell applications are available.

In this article, we report the influence of ZnONF$_S$ and ZnONF$_K$ as an alternative light trapping scheme for nanostructured a-Si TFSCs. Surface morphologies of various ZnONF$_S$ and ZnONF$_K$ with and without H-doping along with optical transmittance and haze ratio are discussed. The sheet resistance, XRD patterns and TEM spectra of ZnONF$_S$ and ZnONF$_K$ deposited on FTO glass have been explained. Roughness profile and 3-D surface morphology

of ZnONF$_K$ are presented. ZnONF$_S$ and ZnONF$_K$ are speculated to have a high haze ratio accompanying excellent light trapping effect which can be applied for high efficiency commercial a-Si solar cells.

2. Experimental details

ZnONF$_S$ and ZnONF$_K$ were grown on the FTO substrate via a solution-based method. Prior to the growth, the substrates were cleaned by rinsing with acetone, methanol and DI water and drying by nitrogen. The seed solution was prepared by dissolving 5 mM of Zn(CH$_3$COO)$_2 \cdot$ 2H$_2$O and 5 mM of KOH in anhydrous ethanol and stirred for 10 min. The seed solution was drop casted onto a FTO glass and placed on a hotplate at 150 °C for 30 min to achieve good adhesion between the seed layer and FTO surface.

To grow ZnONF$_K$, an aqueous solution of 5 mM Zn (CH3COO)$_2 \cdot$ 2H$_2$O was added to 40 mM of NaOH and stirred in an ice bath for 15 min. The seeded FTO substrate was then dipped into the precursor solution for 30 min and placed in a Teflon-lined stainless steel autoclave and heated at 90 °C for 4 h. The as-grown ZnONF$_K$ was then washed with DI water and annealed at 150 °C for 2 h.

For growing ZnONF$_S$, the ZnO nanorods backbones were grown. For ZnO nanorods, first, 0.025 M of hexa-methylene-tetramine (HMTA) and 0.1 M poly-ethylenimine (PEI) were mixed and the resulting solution was added to 0.025 M of Zn (NO3)$_2 \cdot$ 6H$_2$O aqueous solution and stirred for 30 min. The seeded FTO glass was then dipped into the precursor solution, followed by hydrothermal process at 60–90 °C for 7–15 h. The length and diameter of ZnO nanorods arrays could be controlled by altering reaction time, temperature and concentration of precursor solution. These as-grown ZnO nanorods arrays were thoroughly rinsed with DI water and dried by nitrogen gas. ZnO nanorods arrays on FTO glass were finally annealed at 350 °C in ambient air for 10 min for removal of residual organics (mostly PEI). To grow ZnONF$_S$, ZnO nanorods were grown as branches onto the ZnO nanorods array trunks, ZnO nanoparticle seed solution was first added onto the surface of the
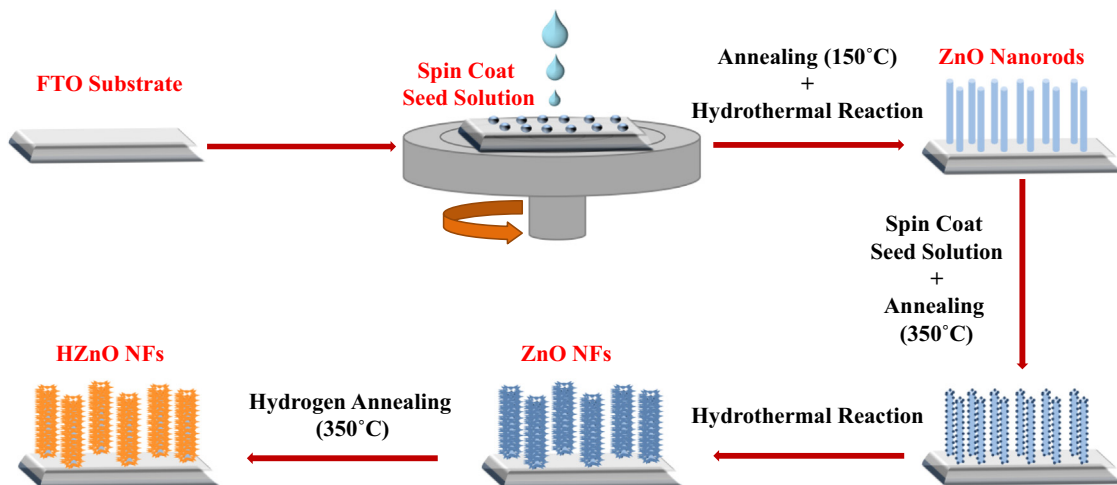

Fig. 1. Schematic of the growth process of ZnO nanoflowers.

as-prepared ZnO nanorods arrays by drop casting and placed on a hotplate at 150 °C for drying for 10 min and subsequently a hydrothermal reaction was conducted as described above without adding ammonia or PEI. Finally, hydrogen doped $ZnONF_S$ and $ZnONF_K$ were obtained by

annealing in hydrogen atmosphere at 350 °C for 3 h. Fig. 1 shows the schematic of the growth of $ZnONF_S$.

The surface morphology of $ZnONF_S$ and $ZnONF_K$ was measured by the scanning electron microscope (SEM JEOL 7610 at 15 kV) system. The X-ray diffraction (XRD) analysis of $ZnONF_S$ and $ZnONF_K$ was performed by using rigaku smart lab XRD (45 kV, 200 mA, Cu K_α) system on glass substrate. The optical characteristics (total, diffused transmittance) were measured by using the solar cell spectral response (QE/IPCE QEX7) measurement system. A 3-D alpha step profiler (Dektak XT) system was used to measure the rms roughness and 3-D surface morphologies of $ZnONF_K$ deposited on the FTO glass. The haze ratio of $ZnONF_S$ and $ZnONF_K$ was defined as the ratio of diffused to total transmittance. Sheet resistance of the $ZnONF_S$ and $ZnONF_K$ was measured by the four probe (CMT-series) system. Transmission electron microscopic (TEM) analysis was performed by using (JEOL, ARM200F at 200 kV) system. TEM samples were prepared by mild sonication of as grown $ZnONF_K$ on FTO substrate immersed in ethanol and subsequently drop casted on the carbon grid.

3. Results and discussion

XRD patterns of $ZnONF_S$ and $ZnONF_K$ deposited with and without H-doping are shown in Fig. 2. The baseline
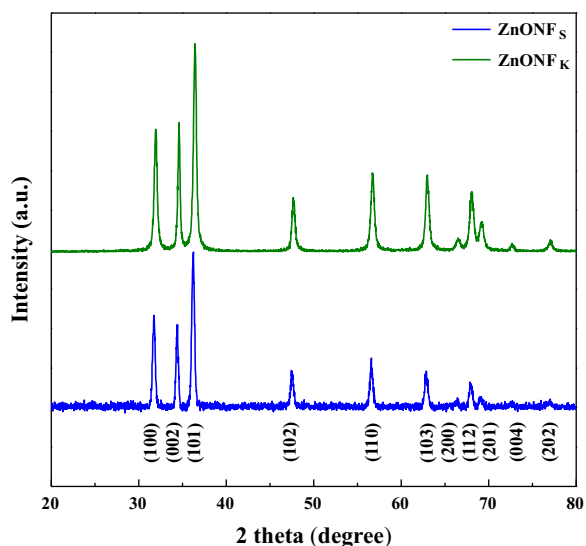

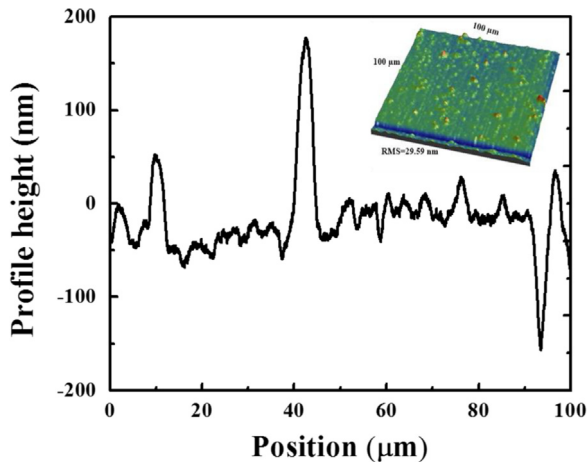Fig. 2. X-ray diffraction (XRD) patterns of ZnO nanoflowers and nanoflakes.
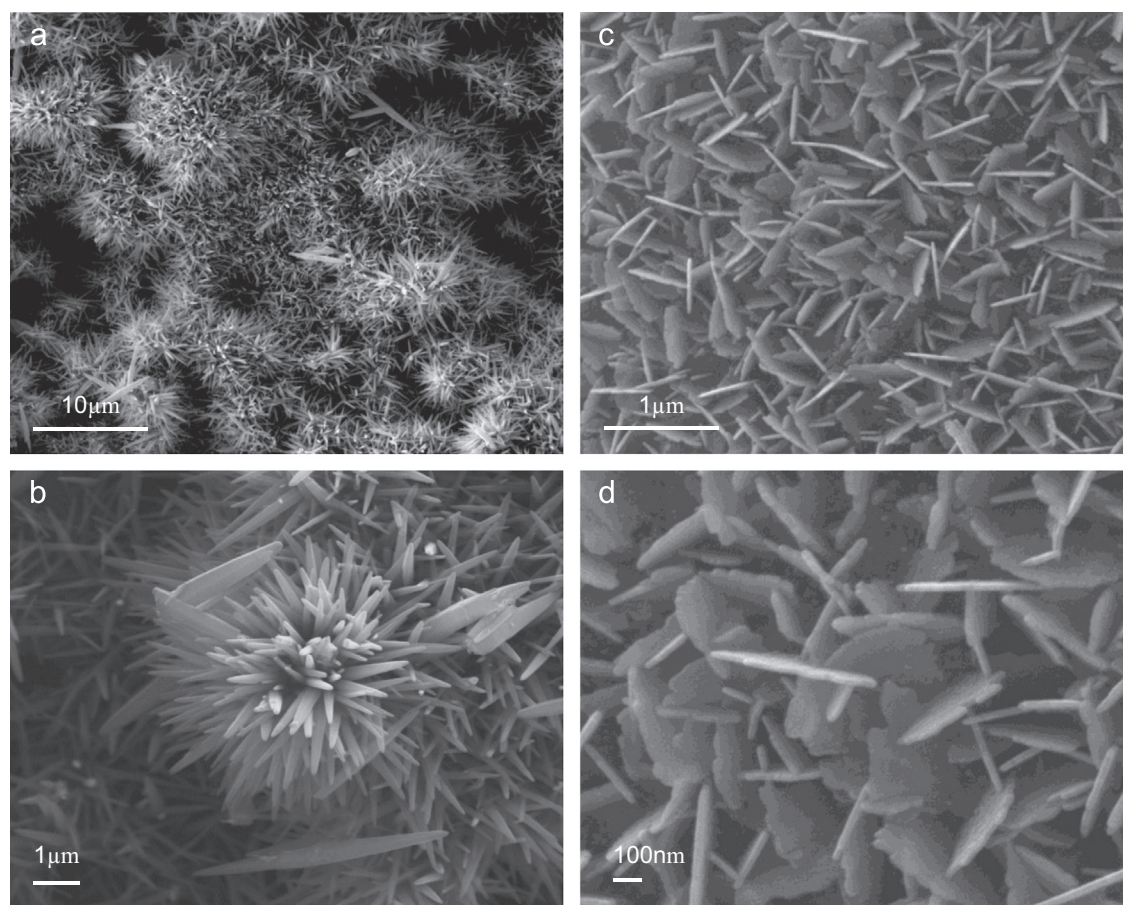
Fig. 3. SEM Images of (a), (b) ZnO nanoflowers and (c), (d) ZnO nanoflakes.

Fig. 4. Profile height image of the ZnO nanoflakes.

Fig. 5. Transmission electron microscopic (TEM) image of ZnO nanoflakes.

substrate for the fabrication of $ZnONF_S$ and $ZnONF_K$ was FTO glass. The XRD diffraction peaks were indexed to the wurtzite structure of ZnO (JCPDS Card no. 65-3411) and by comparing them with the already published results [25–28]. XRD pattern of $ZnONF_S$ and $ZnONF_K$ reveals high degree of crystallinity with preferred orientation along the (100), (002) and (101) planes. The strong and sharp diffraction peaks of ZnO indicate high crystallinity of the samples. Few other prominent peaks corresponding to wurtzite structure of $ZnONF_S$ and $ZnONF_K$ like (102), (110) and (103) were also present.

The surface morphology of $ZnONF_S$ and $ZnONF_K$ is shown in Fig. 3. $ZnONF_S$ were grown on FTO glass using various potassium hydroxide (KOH) concentrations. The length and diameter of nanorods could be controlled by altering the reaction time, temperature and concentration of the precursor. The amount and duration of KOH play an important role on surface morphology of ZnO. Surface morphologies of $ZnONF_S$ are shown in Fig. 3(a) and (b). $ZnONF_S$ like structure was constructed by combining various ZnO nanorods structures with an average diameter of 400 nm and length around 2 μm (~Aspect ratio 5). The diameter and length of ZnO nanorods could be controlled by the concentration of KOH. It is clearly seen that high density $ZnONF_S$ and $ZnONF_K$ are uniformly grown on FTO glass. $ZnONF_S$ have very thin walls with a height of 600–700 nm and thickness of 15–20 nm as shown in Fig. 3(c) and (d) respectively. Due to high roughness and haze ratio [15], $ZnONF_S$ and $ZnONF_K$ can be used for the light trapping in a-Si thin film solar cells [29].

Fig. 4 shows the height profile and inset 3-D alpha step profiler image of the $ZnONF_S$. The surface area of (100×100) μm^2 was scanned to observe the roughness and 3-D surface morphology of the $ZnONF_K$. The rms roughness of $ZnONF_K$ was recorded as 29.59 nm. The profile height showed excellent agreement with the 3-D profiler images of $ZnONF_K$ surface morphology. The evidence of $ZnONF_K$ can be clearly seen from the 3-D surface morphology [30–32].

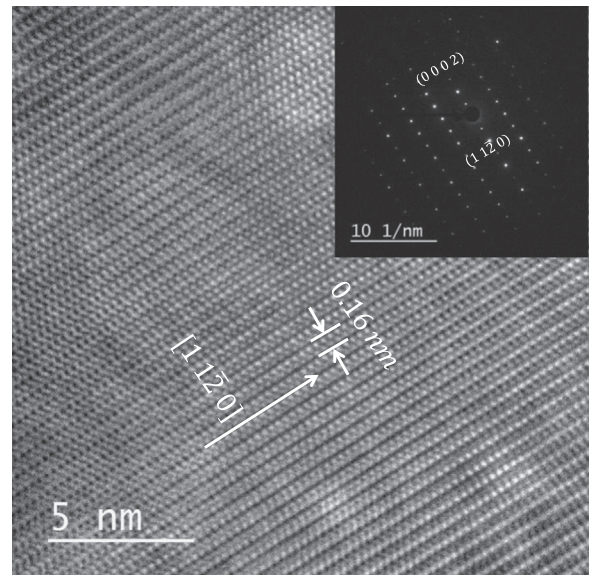The high resolution transmission electron microscope image of $ZnONF_K$ structure is shown in Fig. 5, inset shows the corresponding selected area electron diffraction pattern (SEAD) of lattice image. SAED of a single $ZnONF_K$ confirmed single crystalline growth along ZnO (0002) direction with interlayer distance of 0.16 nm. Although the film exhibited polycrystalline nature as revealed in XRD pattern in Fig. 2. The TEM images also revealed that the $ZnONF_K$ were high-quality single crystal without any visible defects within the area of observation [33,34].

Fig. 6(a) shows the total and diffused transmittance of $ZnONF_S$ and $ZnONF_K$ with and without H-doping. An average transmittance of about 81.77% in the visible wavelength (400–800 nm) range was obtained for as deposited FTO glass. $ZnONF_S$ with and without H-doping showed an average total transmittance of about 82.53% and 83.98% in the visible wavelength region. The total transmittance of the $ZnONF_K$ with and without H-doping was recorded to be 84.766% and 83.06% respectively. The diffused transmittance of as deposited FTO glass was 10.78% in the visible wavelength region. Since H-doping reduces the surface area of the $ZnONF_S$ and $ZnONF_K$, an enhancement in diffused transmittance was observed by H-doping. The diffused transmittance of 26.01% and 33.26% was shown by the $ZnONF_S$ and $ZnONF_K$ with H-doping. Fig. 6(b) shows the haze ratio of $ZnONF_S$ and $ZnONF_K$ with and without H-doping. The haze ratio of ZnO is defined as the ratio of diffused to total transmittance [3,35]. The haze ratio of 13.48% was shown by the as deposited FTO glass while it was decreased from 32.30% to 27.41% for $ZnONF_S$ with and without H-doping. The haze ratio of 40.60% and 22.24% was shown by the $ZnONF_K$ with and without H-doping.

Table 1 represents the sheet resistance of $ZnONF_S$ and $ZnONF_K$ with and without H-doping. Lower sheet resistance of front TCOs is basic requirement for the fabrication of a-Si thin film solar cell. The sheet resistance of as deposited FTO glass was recorded as 8.079 Ω/□ while those for the $ZnONF_S$ with and without H-doping was
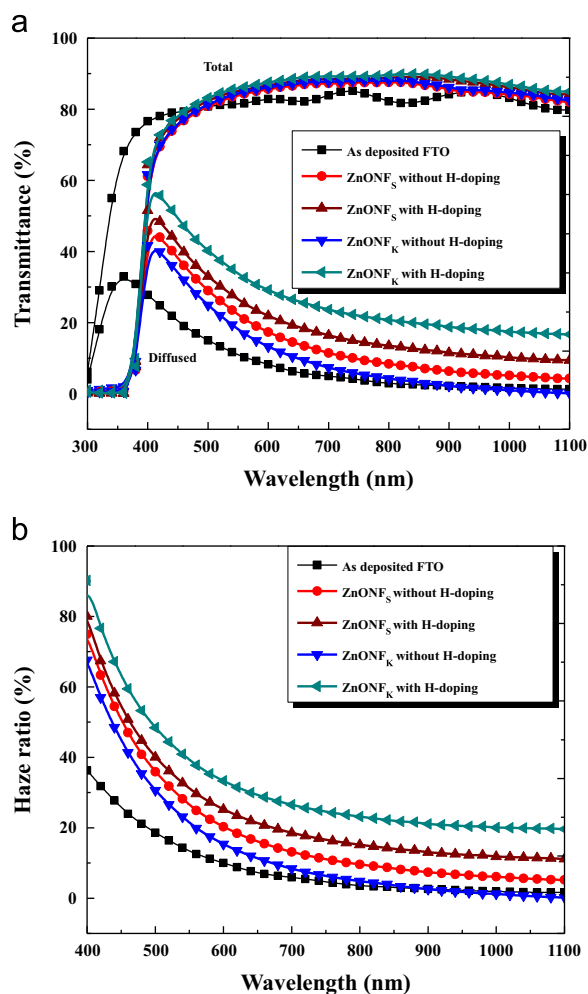
Fig. 6. Optical characteristics (a) total, diffused transmittance and (b) Haze ratio of ZnO nanoflowers and nanoflakes with and without H-doping.

Table 1
Sheet resistance of ZnO nanoflowers and nanoflakes with and without H-doping.

Sample #	Growth condition	Sheet resistance ($\Omega/\square$)
1	As deposited FTO Glass	8.079
2	ZnONF$_S$ without H-doping	7.926
3	ZnONF$_S$ with H-doping	7.896
4	ZnONF$_K$ without H-doping	7.543
5	ZnONF$_K$ with H-doping	7.345

recorded as 7.896 $\Omega/\square$ and 7.926 $\Omega/\square$, respectively. On the other hand, the sheet resistance of ZnONF$_K$ was recorded to be 7.345 $\Omega/\square$ and 7.543 $\Omega/\square$ with and without H-doping, respectively. A minor decrease in sheet resistance of ZnONF$_S$ and ZnONF$_K$ was related to H-doping and higher order of crystallinity since it can enhance the carrier concentration [22–24]. Therefore, the uniform hydrothermally deposited ZnONF$_S$ and ZnONF$_K$ with high haze ratio pave new alternatives to increase the light scattering in nanostructured and a-Si thin film solar cells.

4. Conclusion

In summary, low cost, large area hydrothermally deposited ZnONF$_S$ and ZnONF$_K$ with low sheet resistance and high haze ratio are presented. FTO glass was used as a baseline substrate for the growth of ZnONF$_S$ and ZnONF$_K$ with various aspect ratios. The electrical conductivity and haze ratio of the ZnONF$_S$ and ZnONF$_K$ were enhanced by annealing in hydrogen atmosphere at 350 °C. The XRD patterns of ZnONF$_S$ and ZnONF$_K$ showed strong and sharp peaks of ZnO indicating a higher order of crystallinity. There was an agreement between the roughness profile and 3-D surface morphology of ZnONF$_K$ as measured by alpha step profiler. ZnONF$_S$ and ZnONF$_K$ showed high haze ratio compared to the commercially available FTO films. Due to scale up at low cost, hydrothermally grown ZnONF$_S$ have been proposed for the future light trapping schemes in nanostructure and a-Si thin film solar cells.

References

[1] A. Hongsingthong, T. Krajangsang, A. Limmanee, K. Sriprapha, J. Sritharathikhun, M. Konagai, Thin Solid Films 537 (2013) 291–295.
[2] A. Hongsingthong, T. Krajangsang, I.A. Yunaz, S. Miyajima, M. Konagai, Appl. Phys. Express 3 (2010) 051102–051104.
[3] S.Q. Hussain, S. Ahn, H. Park, G. Kwon, J. Raja, Y. Lee, N. Balaji, H. Kim, A.H.T. Le, J. Yi, Vacuum 94 (2013) 87–91.
[4] T. Kawashima, T. Ezure, K. Okada, H. Matsui, K. Goto, N. Tanabe, J. Photochem. Photobiol. A 164 (2004) 199–202.
[5] K. Mahmood, H.W. Kang, S.B. Park, H.J. Sung, ACS Appl. Mater. Interfaces 5 (2013) 3075–3084.
[6] K. Mahmood, H.J. Sung, J. Mater. Chem. 2 (2014) 5408–5417.
[7] V. Bhosle, J.T. Prater, F. Yang, D. Burk, S.R. Forrest, J. Narayan, J. Appl. Phys. 102 (2007) 023501–023506.
[8] A. Hongsingthong, T. Krajangsang, B. Janthong, P. Sichanugrist, M. Konagai, Proceedings of the 37th IEEE on Photovoltaic Specialists Conference (PVSC), (2011) 000791–000794.
[9] H. Park, J. Lee, H. Kim, D. Kim, J. Raja, J. Yi, Appl. Phys. Lett. 02 (2013) 191602–191604.
[10] R. Yu, C. Pan, Z.L. Wang, Energy Environ. Sci. 6 (2013) 494–499.
[11] Z.L. Wang, J. Song, Science 312 (2006) 242–246.
[12] F.H. Chu, C.W. Huang, C.L. Hsin, C.W. Wang, S.Y. Yu, P.H. Yeh, Nanoscale 4 (2012) 1471–1475.
[13] R. Shi, P. Yang, X. Dong, Q. Ma, A. Zhang, Appl. Surf. Sci. 264 (2013) 162–170.
[14] R.E. Nowak, M. Vehse, O. Sergeev, K. von Maydell, C. Agert., Sol. Energy Mater. Sol. Cells 125 (2014) 305–309.
[15] N.K. Hassan, M.R. Hashim, Y. Al-Douri, Optik 125 (2014) 2560–2564.
[16] T. Premkumar, Y.S. Zhou, Y.F. Lu, K. Baskar, ACS Appl. Mater. Interfaces 2 (2010) 2863–2869.
[17] B. Xiang, P. Wang, X. Zhang, S.A. Dayeh, D.P.R. Aplin, C. Soci, Nano Lett. 7 (2006) 323–328.
[18] S. Dai, Y. Li, Z. Du, K.R. Carter, J. Electrochem. Soc. 160 (2013) 156–162.
[19] A. Umar, M. Akhtar, A.A. Hajry, M.S.A. Assiri, N.Y. Almehbad, Mater. Res. Bull. 47 (2012) 2407–2414.
[20] B. Kilic, T. Günes, I. Besirli, M. Sezginer, S. Tuzemen, Appl. Surf. Sci. 318 (2014) 32–36.
[21] X. Lu, G. Wang, S. Xie, J. Shi, W. Li, Y. Tong, Chem. Commun. 48 (2012) 7717–7719.
[22] G. Chris, V.D. Walle, Phys. Rev. Lett. 85 (2000) 1012–1015.
[23] G. Chris, V.D. Walle, Physics B 308–310 (2001) 899–903.

[24] P. Yang, X. Xiao, Y. Li, Y. Ding, P. Qiang, X. Tan, W. Mai, Z. Lin, W. Wu, T. Li, H. Jin, P. Liu, J. Zhou, C.P. Wong, Z.L. Wang, ACS Nano 7 (2013) 2617–2626.
[25] I.Y.Y. Bu, C.C. Yang, Superlattice Microstruct. 51 (2012) 745–753.
[26] N.T.H. Trang, H.V. Ngoc, N. Lingappan, D.J. Kang, Nanoscale 6 (2014) 2434–2439.
[27] M. Zareie, A. Gholami, M. Bahram, A.H. Rezaei, M.H. Keshavarz, Mater. Lett. 91 (2013) 255–257.
[28] L. Zhang, Y. Yin, Sens. Actuator B: Chem. 183 (2013) 110–116.
[29] Z. Liang, R. Gao, J.L. Lan, O. Wiranwetchayan, Q. Zhang, C. Li, Sol. Energ. Mat. Sol. C. 117 (2013) 34–40.
[30] M.L. Addonizio, A. Spadoni, A. Antonaia, Appl. Surf. Sci. 287 (2013) 311–317.
[31] F.H. Wang, C.F. Yang, Y.H. Lee, Nanoscale Res. Lett. 9 (2014) 97–103.
[32] W.T. Yen, Y.C. Lin, J.H. Ke, Appl. Surf. Sci. 257 (2010) 960–968.
[33] S.H. Lee, K. Fujii, T. Minegishi, T. Yao, J. Korean Phys. Soc. 53 (2008) 406–411.
[34] X. Zhang, J. Qin, Y. Xue, P. Yu, B. Zhang, L. Wang, Sci. Rep. 4 (2014) 4596–4603.
[35] S.Q. Hussain, S. Kim, S. Ahn, N. Balaji, Y. Lee, J.H. Lee, J. Yi, Sol. Energ. Mat. Sol. C. 122 (2014) 130–135.